Near-wake structure behind two circular cylinders in a side-by-side configuration with heat release

S. Kumar, G. Laughlin, and C. Cantu
Department of Engineering, The University of Texas at Brownsville, Texas 78520, USA
(Received 2 June 2009; revised manuscript received 1 October 2009; published 10 December 2009)

Flow around two circular cylinders in a side-by-side arrangement normal to the free stream with heat release from one of the cylinders is studied experimentally. This flow, *with no heat release*, is known to exhibit a range of flow regimes at different cylinder spacings. In particular, the wake exhibits well-known intermittently bistable behavior in the center-to-center spacing (normalized by cylinder diameter) range of 1.2–2.0. We present, for the first time, the effect of heat release from *one of the cylinders* on the near-wake structure of the two cylinder configuration. The experiments are performed at spacing ratios of 1.1, 1.7, and 3.0, Reynolds numbers of 250, 350, and 450 and Richardson number less than 0.14. The investigations are carried out in a water tunnel using hydrogen bubble technique for flow visualization and particle-image-velocimetry for quantitative measurements. The bistability of the wake at a spacing ratio of 1.7 is controlled with a threshold heat release from one of the cylinders resulting in a stable narrow wake behind the heated cylinder and a wider wake behind the unheated cylinder. The heat release resulted in deflection of the gap-bleeding flow toward the heated cylinder at spacing ratio of $S/D=1.1$ and did not produce any visual changes in the near-wake structure at spacing ratio of 3.0.

DOI: 10.1103/PhysRevE.80.066307 PACS number(s): 47.32.Ff, 47.32.ck

I. INTRODUCTION

Flow around bluff bodies is a classical problem of considerable practical importance. Such flows have direct applications in engineering problems such as flow induced oscillations and acoustic noise generation, among others. The complexity of the problem has been correctly pointed out by Roshko [1] in the opening lines of his paper as "…the problem of bluff body flow remains almost entirely in the empirical, deceptive realm of knowledge. What knowledge has been accumulated is in fact impressive…." The canonical problem for studying such flows is the flow around circular cylinders. Flow around a single circular cylinder has now been studied for almost a century and considerable knowledge on the wake structure has been gained at various Reynolds numbers ($\mathrm{Re}=U_\infty D/\nu$). In the definition of Reynolds number D is the cylinder diameter, U_∞ the freestream velocity, and ν the kinematic viscosity. In the last few decades, attention has also been focused on the study of flow around two circular cylinders in a side-by-side arrangement. This arrangement of circular cylinders represents one of the simplest arrangements for studying flow around multiple bluff bodies.

Flow around multiple cylinders finds applications in problems such as heat exchanger flows, flow around power lines, and screens, among several others. Flow around such arrangements of cylindrical structures is very complex involving interactions of separated shear layers, boundary layers, and shed vortices. The flow around two circular cylinders in a side-by-side arrangement is a first step in understanding the flow around multiple cylinders. This flow has been studied extensively in the past, such as, by Bearman and Wadcock [2], Zdrakowich [3], Williamson [4], Sumner *et al.* [5], and Wang and Zhou [6] among several others. The flow exhibits a range of flow regimes (i.e., the morphology of the wake structure) as the spacing between the cylinders is varied, keeping all other parameters of the flow (such as Reynolds number) constant. The spacing is characterized by a nondimensional number, S/D, where S is the center-to-center spacing.

The wake structure of the flow around two circular cylinders in a side-by-side arrangement is classified into three categories independent of the Reynolds number [6]. The categories are based on the value of the spacing parameter, S/D. The different ranges of S/D for each category are $S/D<1.2$, $1.2<S/D<2.0$, and $S/D>2.0$. In the range $S/D>2.0$ (i.e., the cylinders being relatively far apart) two separate Karman Vortex streets, one behind each cylinder, are formed. The two streets are coupled with a definite phase relationship [7] and single shedding frequency [8]. The vortex shedding frequency in this regime behind either of the two cylinders matches with the shedding frequency behind a single cylinder wake experiment. Ishigai [9] observed symmetric vortex street for $S/D=2.5$ and 3.0 using schlieren optical diagnostics. Williamson's [4] flow visualization experiments at Reynolds numbers of 100–200 and $2<S/D<6$ showed that the two coupled vortex streets can occur both in in-phase and in antiphase mode which correspond to, for example, asymmetrical or symmetrical shedding, respectively, about the centerline between the two cylinders along the flow direction.

The range $S/D<1.2$ corresponds to the cylinders being relatively very close to each other. The flow behaves almost like the flow around a single bluff body in this case. Vortices are shed from the outer sides of the two cylinders resulting in a single vortex street. The shedding is alternate but is sometimes modified to symmetric shedding as noted by Sumner *et al.* [5]. There is no vortex shedding from the gap between the cylinders but there is a flow in the gap between the two cylinders called as the "gap-bleeding" flow. Sumner *et al.* [5] associated the gap-bleeding flow with higher momentum fluid which increases the base pressure, reduces the drag of

 ©2009 The American Physical Society

both cylinders, and increases the streamwise extent of the vortex formation region.

The flow in the spacing range of $1.2 < S/D < 2.0$ exhibits interesting intermittently bistable behavior. The flow between the two cylinders is called as the "gap-flow." There is a distinct vortex street from each cylinder with a strong coupling between the two. The wake behind one of the two cylinders can be narrower or wider than the one behind the other depending on whether the direction of gap-flow deflection is toward or away from the cylinder. The vortex shedding frequency in the narrow wake is known to be about three times the one behind the wide wake [2]. The gap flow between the two cylinders behaves in an intermittently bistable manner independent of the Reynolds number [7]. This intermittently bistable behavior results in an alternating narrow and wide wake behind one of the two cylinders in an unpredictable manner. Wang and Zhou [6] alluded to a possible mechanism for the bistable behavior of the wake. The mechanism is related to the phase difference between the two vortices in the gap flow. The gap vortex in the narrow wake lags behind the gap vortex in the wide wake and the shifting of the wake, i.e., wider wake becoming narrower and narrow wake becoming wider is triggered by some perturbation which reverses the phase relationship between the two vortices. This is schematically shown by a sketch in Fig. 14 of Wang and Zhou's [6] paper.

The control of the near-wake structure behind two cylinders in the bistable regime at $S/D=1.75$ was attempted by Kim and Durbin [7] using acoustic excitations and placement of a splitter plate. The acoustic excitations were able to make the flow symmetric in the mean when the natural flow without the excitation was highly asymmetric due to gap-flow deflection. The positioning of the splitter plate at appropriate locations between the two cylinders helped in achieving the symmetrical wake pattern. There has been no attempt, to the best of our knowledge, to understand the response of the near-wake structure of the two cylinder configuration to the heat release. There have been some recent studies [10–15] on the flow around a single heated cylinder. The focus of these experimental and numerical studies has been mainly to understand the effect of heat release on the near and far wake structure. These studies also focus on the onset of vortex shedding and the Reynolds number-Strouhal number relationship for a single cylinder. The effect of heat release on the near-wake structure of a single oscillating circular cylinder was extensively studied by Pottebaum [16].

The present experimental study focuses on the effect of heat release from *one of the cylinders* on the near-wake structure behind two cylinders. The schematic of the problem is shown in Fig. 1. The heating is limited so that the effects of buoyancy and free convection can be neglected. The experiments are done at $S/D=1.1$, 1.7, and 3.0 at $\mathrm{Re}=250$, 350, and 450. Special attention is focused on the spacing ratio of $S/D=1.7$ which was also the subject of investigation by Wang and Zhou [6] where the wake behaves in an intermittently bistable manner without heat release. We were particularly interested in answering the questions: what is the effect of heat release on the bistability of the wake? How does it change the near-wake structure? The answer to these questions can be very important from the flow-control point of view.

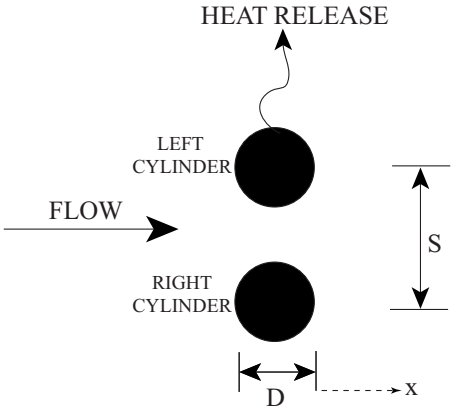

FIG. 1. Schematic of the problem.

II. EXPERIMENTAL SETUP AND DIAGNOSTICS

The experiments for this study were carried out in a water tunnel (Rolling Hills Inc.: model 0710) with a test section of depth 0.25 m, length 0.46 m, and width 0.18 m. The tunnel has a return circuit to recirculate the water using a 1.5 hp variable speed centrifugal pump. The sides of the test section are made of 6 mm thick tempered glass. The maximum speed of the flow can be 0.13 m/s and the turbulence intensity is less than 0.5% rms. The top of the tunnel test section is open and hence a rectangular piece of glass of size $475 \times 184 \times 3$ mm^3, with a 75×7 mm^2 wide slot in the middle was placed on top of the test section. The two cylinders mounted on a traverse mechanism were inserted from above through the slot in the glass cover and spanned the full depth of the tunnel. During the experiments, the water level was touching the glass surface. Since the experiments involved heat release from the circular cylinders, the free-stream water temperature was maintained constant at 21 °C using a Neslab Coolix 2200 chiller connected to the tunnel. The water from the tunnel was recirculated through the chiller to maintain the water temperature constant. The temperature of the free-stream flow was monitored by a thermometer.

The two cylinders used in the experiment were custom cartridge heaters manufactured by Watlow (part number E14A-11355). The cylinders consisted of a thin coil of high resistivity surrounded by compact magnesium oxide insulator and encased in a 304-stainless steel sheath. The length and outer diameter of each of the two cylinders was 366 mm and 6.35 mm, respectively. The resistor leads protrude from one end of the cylinder. The bottom 5 mm and top (near the leads) 157 mm of the cylinders were unheated portions leaving 204 mm as the heated length. The cylinders were mounted on a fixture and inserted from the top of the tunnel with the leads, from the end of the cylinder, coming out of the tunnel. The fixture was designed to hold the cylinders vertically and be able to move them in spanwise (perpendicular to the flow) direction to change the spacing, S/D. The blockage resulting from the two cylinders in the tunnel was 7.1%. It is emphasized that only one of the cylinders was heated. The flow diagnostics was done in a horizontal plane at 140 mm from the bottom of the cylinder. The schematic of a heated cylinder is shown in Fig. 2.

FIG. 2. Schematic of the heated cylinder.

The cylinder was heated by a variable voltage dc power supply (Kikusui PAN 250–2.5A) for the experiments at Re =250, 350, and 450. The average surface temperature of the heated cylinder in water at the three Reynolds number was measured by measurements with a J-type thermocouple mounted on the downstream side of the heated cylinder surface. The diameter of the wires used to make the thermocouple junction was 0.13 mm. A very thin (10–15 μm) film of bonding silicone (LOCTITE 5145 with thermal conductivity of 0.2 W/m K) was applied on the downstream cylinder surface, along the length, on a area of about 2 mm wide and 230 mm length. The thermocouple junction was bonded on this film at a distance of 140 mm from the end of the cartridge cylinder. A similar film was applied on top of the junction to prevent contact with tunnel water. The thermocouple junction was calibrated with a calibrated thermocouple probe. The surface temperature measurements made with the thermocouple in the two cylinder configuration at spacing of $S/D=1.7$ and maximum value of heat release, gave a *difference* in temperature from the free-stream water temperature, of 10, 20, and 24 °C at Re=250, 350, and 450, respectively. The Richardson number $\mathrm{Ri}=\mathrm{Gr}/\mathrm{Re}^2$, where $\mathrm{Gr}=g\beta(T_W-T_\infty)D^3/\nu^2$, was used as a parameter to determine the criterion for forced convection according to Morgan [17] as $\mathrm{Ri}<0.5$. In the definition for Ri, g is the acceleration due to gravity and β is the volumetric coefficient of thermal expansion, T_W is the cylinder surface temperature, ν, the kinematic viscosity, and T_∞ is the free-stream water temperature. The Ri in the present experiments was less than 0.14 thus justifying the fact that buoyancy and free convection effects can be neglected.

The schematic of the experimental setup is shown in the Fig. 3. The schematic is representative of both the flow visualization and particle-image-velocimetry (PIV) experiments. The flow visualization was done using the hydrogen bubble technique. This was implemented with a 25 μm diameter platinum wire, acting as cathode, stretched across the width of the test section 5 mm upstream of the cylinders and a small graphite plate, acting as anode, placed downstream.

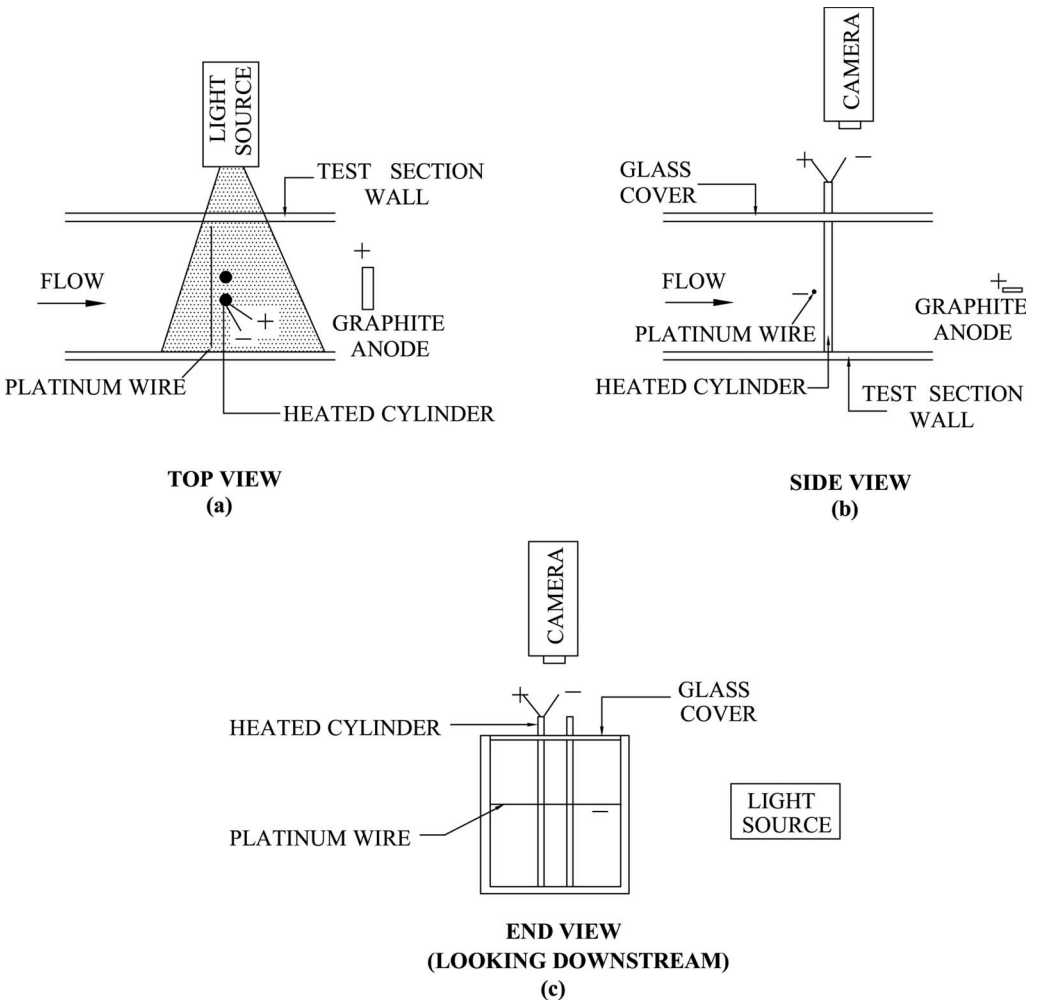

FIG. 3. Schematic of the experimental setup for flow visualization and PIV experiments. (a) Top view; (b) side view; (c) end view. *Platinum wire and graphite anode were absent for PIV studies.*

The platinum wire was soldered on the tip of two brass prongs of 1.5 mm diameter. A graphite plate ($102\times25\times3.8$ mm^3), with streamlined leading and trailing edge, was placed about 406 mm downstream from the platinum wire in the same horizontal plane as the wire. A variable voltage dc power supply (Kikusui PAN 250–2.5A) was used to apply a potential difference between the graphite plate (positive) and the platinum wire (negative). Potential difference of about 12–14 V was sufficient to obtain good quality hydrogen bubbles in the present experiments. A small amount (~40 g) of sodium sulfate was added to the water in the tunnel to facilitate the electrolysis. The hydrogen bubbles formed on the platinum wire are swept downstream by the flow to form a sheet of bubbles. The bubble sheet was illuminated from the side by an overhead projector (model 3M-9100). The flow structures, made visible by the illuminated bubble sheet, were captured by a still image charge-coupled device (CCD) camera (Model: Apogee U260, CCD 512×512 pixel). The camera was mounted on a traverse mechanism and viewing at right angles to the illumination and flow direction. Motion pictures were also captured at 30 frames/s with a Sony HDR-HC5 digital video recorder mounted at the same location as the still image camera. The framing rate provided sufficient resolution to characterize the flow features at relatively low Reynolds numbers of 250, 350, and 450 in the present experiments.

The PIV measurements were done in the water tunnel in the same experimental conditions (but as different realizations) as the flow visualization experiments. The schematic of the PIV experiments is shown in Fig. 3 with the exception of the platinum wire and the graphite anode, which were absent. The light source and camera were a laser and a PIV camera, respectively. A Dantec PIV system using DYNAMIC-STUDIO v 2.0 platform from Dantec was used to obtain quantitative information on the velocity and the vorticity fields. The flow was seeded with 10 μm diameter silver coated hollow glass spheres. The flow was illuminated in a horizontal plane just downstream of the cylinders with a laser sheet. The laser sheet was formed using the cylindrical lens optics in front of the New Wave laser (model: Solo PIV laser 120 XT—15 Hz). The digital images of the glass spheres (particles) in the plane of the laser sheet were captured using a HiSense-MkII CCD camera for PIV analysis. The size of the captured images was 1340×1024 pixels. The physical area covered by the images was 47×36 mm^2, corresponding to a magnification of about 0.035 mm/pixel. The image processing was done using 32×32 rectangular interrogation areas with 25% overlap in the horizontal and vertical directions. This resulted in the spatial resolution of 0.84 mm [32 pixels$\times(1-0.25)\times$(0.035 mm/pixel)] or $0.132D$ in the vorticity fields. The number of velocity vectors calculated in the imaged area were 55×42, i.e., 2310 vectors. The spanwise vorticity, ω_z, was calculated from these velocity vectors at the same number of places.

III. RESULTS

The experiments were performed at three Reynolds numbers of 250, 350, and 450 and spacing ratios of $S/D=1.1$, 1.7, and 3.0. The choice of these parameters facilitated comparison with Wang and Zhou's [6] work. The spacing ratio of $S/D=1.7$ results in an intermittently bistable wake. The various terms used to describe the wake structure at this spacing of $S/D=1.7$ are clearly identified in the schematic in Fig. 4. The flow visualization data in Fig. 5 shows the near wake (about $\sim13D$ streamwise extent) structure behind two cylinders, with no heat release, at $S/D=1.7$ and Re=350. The data are similar to the work reported by Wang and Zhou [6] using planar-laser-induced fluorescence flow visualization technique.

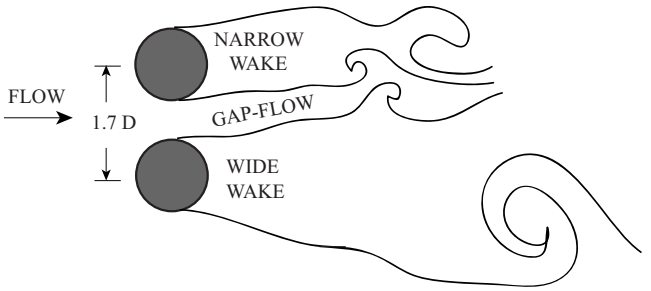

FIG. 4. Schematic of a typical wake structure at $S/D=1.7$.

The gap-flow, various vortical structures and their interactions are clearly captured by the hydrogen bubble technique. Figures 5(a)–5(c) show three instances of the intermittently bistable wake at Re=350 and $S/D=1.7$. In Fig. 5(a) the gap flow is deflected toward the left (looking downstream) resulting in a wider wake toward the right. The two vortices formed on the gap-flow tip and the one on the outer side of the left cylinder merge to form a vortex pair as shown by the label "vortex merger." The rollup of the shear layer

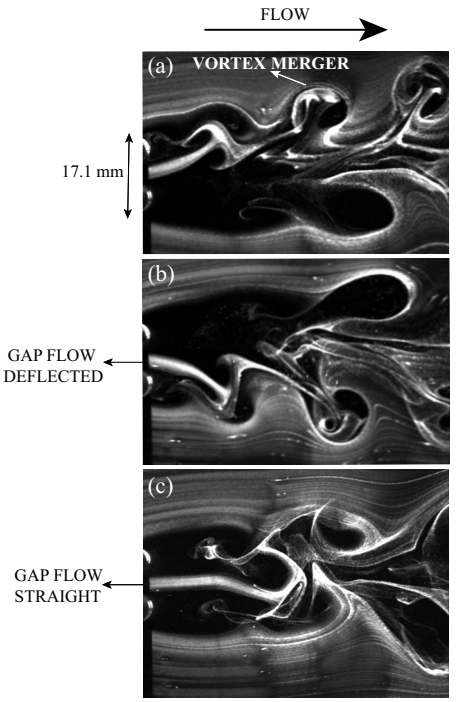

FIG. 5. The near-wake structure behind two *unheated* cylinders at Re=350 and $S/D=1.7$ showing bistable wake behavior. (a) Gap-flow deflection to the left; (b) gap-flow deflection to the right; (c) the intermediate gap-flow position.

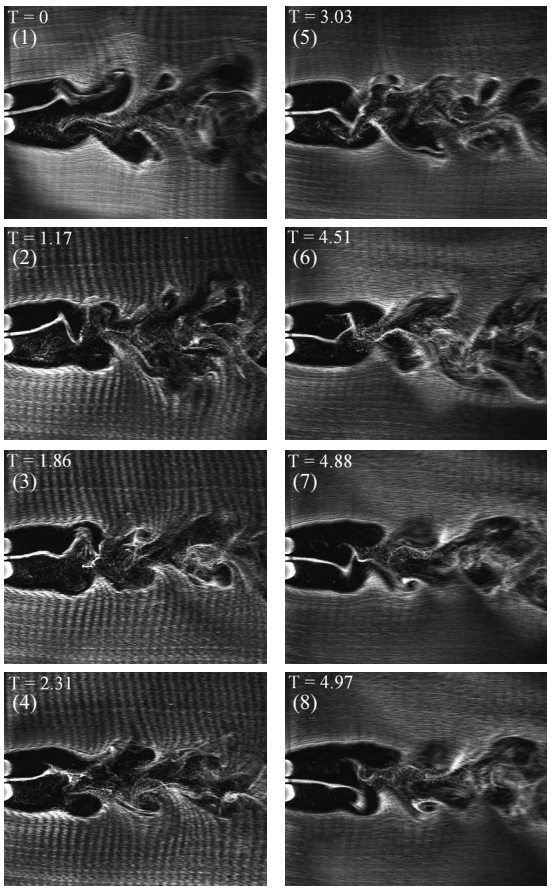

FIG. 6. Sequence of eight frames showing the transition of narrow and wide wake behind unheated cylinders at Re=350 and $S/D=1.7$.

coming off the outer edge of the right cylinder happens later ($\sim x=9D$ downstream from the cylinders) than its counterpart on the left cylinder, i.e., the cylinder which has the narrower wake, where the rollup starts at about $x=3D$. In Fig. 5(b) the gap flow has shifted toward the right cylinder resulting in a narrow wake behind it. The shifting between the two stable states of the wake structures shown in Figs. 5(a) and 5(b) occurs in an intermittent manner, i.e., the narrow wake and the wide wake switched positions randomly. The random intermittent switching between the two states can occur in anywhere from 30 s to as long as 60 min or more as observed in the present experiments. The mean time between shifting of the wide and narrow wake was found by Kim and Durbin [7] to decrease nearly exponentially with increasing Reynolds numbers. At Re=200 Williamson [4] observed a steady mean flow with no random intermittent switching of gap flow. Figure 5(c) shows the wake structure when the gap flow is relatively straight in the beginning and there is no clear "narrow" or "wide" wake behind either of the cylinders. This flow visualization image was captured when the wake structure was switching from one state to the other. The transition process in the switching of the "narrow" and "wide" wake was also captured in the motion picture recorded with a video camera. Figure 6 shows eight frames captured from the motion pictures to show the beginning and end of the switching of narrow and wide wakes.

TABLE I. Table summarizing vortex shedding time period, T_0, for wider wake and corresponding Strouhal numbers, St, at the three Reynolds numbers.

Re	T_0 (s)	St
250	1.84	0.086
350	1.17	0.090
450	0.84	0.108

The times, T, shown on each frame of Fig. 6 represent nondimensional times obtained by normalizing actual time by the vortex shedding period, T_0, of the wide wake at $S/D=1.7$. The physical times in the present paper are nondimensionalized by T_0 for the unheated cylinder case. The vortex shedding period was measured from frame-by-frame analysis of the motion picture, i.e., counting the same sign outer vortices of the wider wake at $x\sim 11D$. Table I shows the values of T_0 and calculated values of corresponding Strouhal numbers of the wider wake at the three Reynolds numbers. Strouhal number is defined as fD/U_∞, where f is the vortex shedding frequency. In the present case, $f=1/T_0$.

The values of Strouhal numbers for wider wake at higher Reynolds numbers are close to the those measured by Wang *et al.* [6] who measured St$\sim$0.1. The transition time for the narrow and wide wake to switch was observed to be close to 6 s in the present experiments. The near-wake morphology and behavior at Re=250, 450 and $S/D=1.7$ was qualitatively similar to the one observed for Re=350 and $S/D=1.7$, i.e., the same intermittent bistable behavior was observed.

The two states of the wake structure observed in the present experiments with unheated cylinders at $S/D=1.7$ are stable states. To study the response of the wake structure in one of the stable states at the three Reynolds numbers, an external perturbation was forced on one of the cylinders. The nature of the external perturbation consisted of the downstream and upstream motion of the cylinder. The cylinder was moved in the downstream direction by 2 mm ($\sim 0.31D$) and then immediately moved upstream to its initial position. The complete upstream and downstream motion lasted for approximately 0.5 s. The schematic of the perturbation motion of the cylinder is shown in Fig. 7. The figure shows the schematic with perturbation applied to the cylinder when it had a wider wake; however, in the experiments the perturbation was applied when the cylinder had either

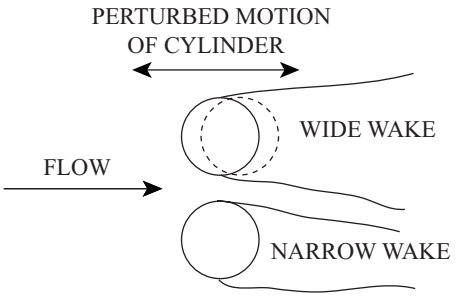

FIG. 7. Schematic of externally perturbed motion of the cylinder at $S/D=1.7$.

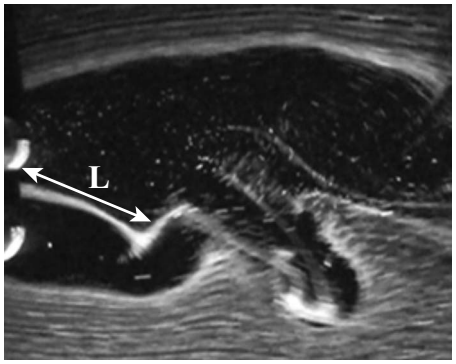

FIG. 8. Illustration of gap-flow length measurement.

wider or narrower wake before perturbation. In the present study, we studied the effect of external perturbation on the evolution of gap-flow length. The gap-flow length was measured from the images captured from the motion pictures and is defined as the length from the location of the two cylinders to the location where the gap flow rolls up into two vortices or shows a sudden bend or a kink. Figure 8 illustrates the definition of gap-flow length, L, for a typical image.

The external perturbation has a very visible and interesting effect on the dynamics of the wake structure at the three Reynolds numbers. The most easily observable effect was visible in the length of the gap flow. The gap flow showed sudden decrease in the length immediately after the perturbation was applied and then returned to its normal oscillating behavior. The perturbation, in some cases, had the effect of switching the wider and narrow wake regions by switching the gap flow. In the present experiments we determined if the gap flow has been stably switched due to perturbation by observing its behavior for 60 s after the perturbation. If the gap flow remained on one side for this time then it was assumed that the perturbation had the effect of stably switching the gap flow. Figure 9 shows the response of gap-flow length to external perturbation at the three Reynolds numbers. The gap-flow length was measured at every 1 s interval to study its evolution with time. The start and end times of the external perturbation is denoted by T_{start} and T_{end}. In the present experiments the same perturbation was applied five times each for Re=250, 350, and 450. It was observed that for Re=250 the gap flow did not switch in a stable manner for five repeated cases of externally applied perturbations but showed oscillations with the size of the two wakes becoming comparable on some occasions. The gap flow at times showed signs of switching but eventually returned to its original side and thereby no stable switching was observed. Similar experiments at Re=350 and 450 showed gap flow stably switching in three of the five cases each. This observation suggests that perhaps the two states might be "more stable" at lower Reynolds numbers. This is also consistent with the observations of Kim and Durbin [7] and Williamson [4] who observed more stability of the gap-flow orientation as the Reynolds number is decreased. The motion pictures [18] of the effect of external perturbation at the three Reynolds numbers of 250, 350, and 450 show the dynamically oscillating behavior of the wake in response to the external perturbation. The movies for Re=350 and 450 show switching of the wide and narrow wakes due to perturbation. In the movie for Re=250 and 350, the perturbation was applied when the perturbed cylinder had a wider wake before perturbation, while for Re=450 it was applied when the same cylinder before perturbation had a narrower wake.

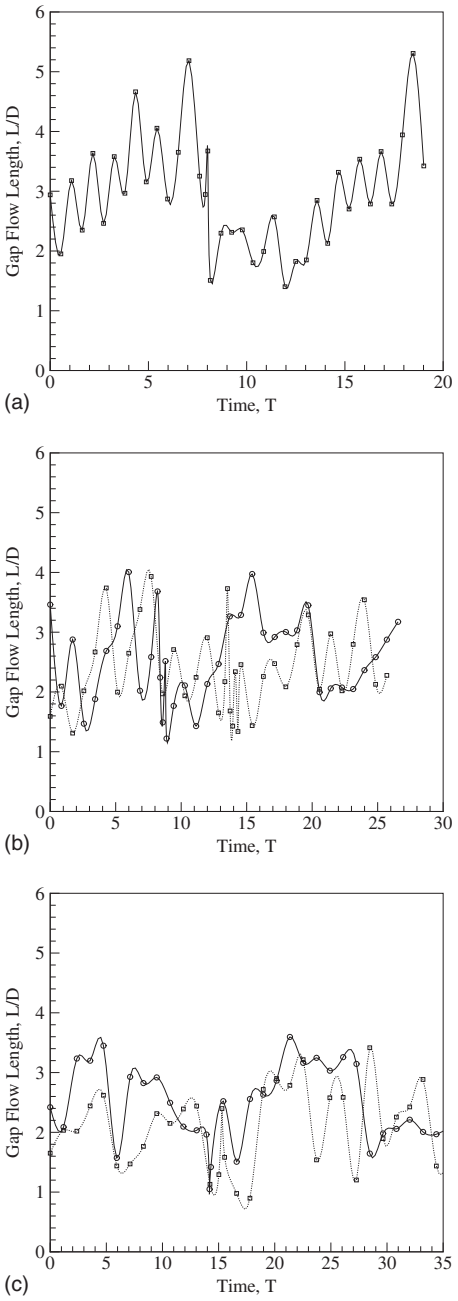

FIG. 9. Evolution of gap-flow length with perturbation at $S/D=1.7$. (a) Re=250, no switch: $T_{start}=7.90$ and $T_{end}=8.15$; (b) Re=350, solid line—switch: $T_{start}=8.2$ and $T_{end}=8.9$, dotted line—no switch: $T_{start}=13.3$ and $T_{end}=14.3$; (c) Re=450, solid line—switch: $T_{start}=13.9$ and $T_{end}=14.4$, dotted line—no switch: $T_{start}=15$ and $T_{end}=15.5$.

The effect of heat release was studied on the bistability of the near-wake structure at Re=350 and $S/D=1.7$ by heating the right cylinder. The attention was focused on the behavior of the gap-flow because the deflection of the gap-flow determined whether the wake behind one cylinder was narrower

or wider than the other. The heat release, in the present experiments, was increased by increasing the current in increments of 0.1 A. At each value of heat release the gap flow was observed for 15 min. It was observed that at low heat releases the gap flow continued to behave in the same intermittently bistable manner as without the heat release. In some cases, the gap flow was stably deflected toward one cylinder for the full observation duration. If the gap flow deflected toward the heated cylinder in between the 15 min observation duration then the same heat release was switched from one cylinder to the other to observe if the gap flow behaved and deflected in the same manner, i.e., if the behavior was *repeatable*. At a threshold value of the heat release, the gap-flow responded to the heat release and switched from one side to the other in about 60 s ($\Delta T=51.4$) and did not switch back for additional 30 min of observation as long as the heat release was present, resulting in a stable narrow wake behind the heated cylinder. The heat release was called a "threshold value" if the behavior of response of gap flow to threshold heat release was observed to be *repeatable*, i.e., by switching the threshold heat release from one cylinder to another, the gap flow switched in 60 s and responded in a similar manner. The intermittently bistable behavior changed to a stable wake structure with a narrow wake behind the heated cylinder. The average temperature of the cylinder surface at this threshold heating condition was estimated from the measured thermocouple reading to be approximately 20 °C higher than the free-stream water temperature of 21 °C.

Figure 10 shows the flow visualization images of the effect of heat release at Re=350 and $S/D=1.7$. The heat release was at the threshold level in these images. Figure 10(a) shows the wake structure with both cylinders *unheated* and the gap flow deflected to the left cylinder. The threshold heat release was then turned ON and the gap flow started deflecting to the heated cylinder. Figure 10(b) shows the condition when the gap flow was in the middle and relatively straight. This condition is not stable and the wake also shows a clearly visible disorganized structure. The wake structure in Fig. 10(b) soon changed to a stable configuration in Fig. 10(c) with gap flow deflected toward the heated cylinder.

The changes in the wake structure resulting from the cylinder heating were also captured in motion pictures. Figure 11 shows eight frames captured from the motion pictures to show the effect of heat release on the wake structure. The frames have been numbered in the order of increasing time. Frame 1 in the figure is with unheated cylinders for comparison. Frame 1 shows the narrow wake behind the left cylinder and in this situation had no tendency to switch. The heat release was then turned ON at this instant on the right cylinder and the time $T=0$ in Frame 2 refers to when the threshold heat release was turned ON. The heated cylinder on the right is not visible in the frames of Fig. 11 because the change in refractive index of water due to heat release in the immediate surrounding of the heated cylinder causes its image to slightly displace upstream, just out of the field of view of the frame. Frames 2 through 10 show the effect of heat release on the near-wake. From frames 2 through 4 ($T=0$ to 36.14) the gap flow is always deflected toward the left cylinder. Frame 5 ($T=41.43$) shows the gap flow straightening

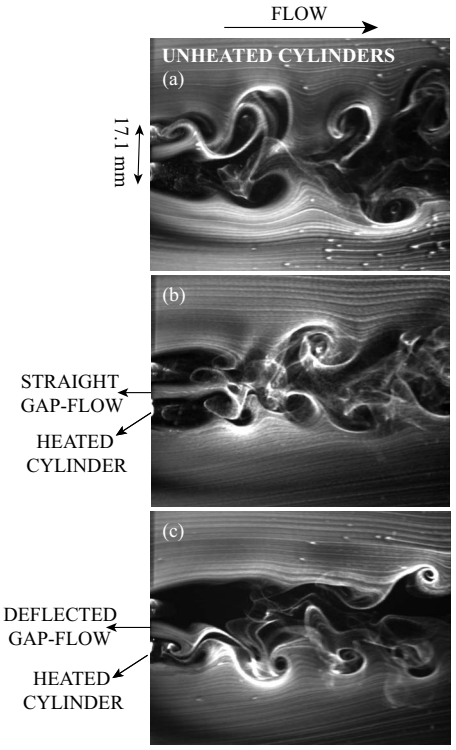

FIG. 10. The near wake behind two cylinders at Re=350 and $S/D=1.7$ showing the effect of threshold heat release. (a) Gap-flow deflection to the left in unheated cylinders; (b) gap flow relatively straight with heat release; (c) the gap-flow forced to the right with heat release.

out and in frame 6 ($T=44.23$) the gap flow is straight with the tip bent toward right. The wakes behind both the cylinders are of comparable size in frame 6. Frame 7 ($T=49.03$) shows the gap flow slightly deflect toward right and in frame 8 ($T=51.73$) the gap-flow has deflected toward the heated cylinder resulting in a narrow wake behind it. Frames 9 and 10 at $T=59.84$ and 1540, respectively, show the wake structure with the gap flow stably deflected toward the heated cylinder. Comparison of frame 1 and frame 10 also shows that the length of the deflected gap flows are of comparable size in the heated cylinder case and the unheated cylinder case. The heat release had the effect of switching the narrow and the wide wake. The heat release was changed from the right to the left cylinder and the gap flow was observed to switch back toward the heated cylinder on the left on the same time scale at the threshold heat release value only (images not shown). The time scale for this forced switching by heat release between the narrow and wide wake was observed to be about 60 s in the present experiments. The behavior of the gap-flow length measured in every 1 s increments in case of stable gap-flow switching, both with no heat release and with threshold heat release is shown in Fig. 12. The length of the gap flow shows oscillations and grows to a maximum length of $\sim 4.5D$ when it is relatively straight and unbiased toward either cylinder. This happens when the gap flow is in the process of shifting from one side to the other.

PIV measurements were made in the intermittently bistable regime of the wake to quantify the distributions of spanwise component of vorticity, ω_z. Figures 13(a) and 13(b)

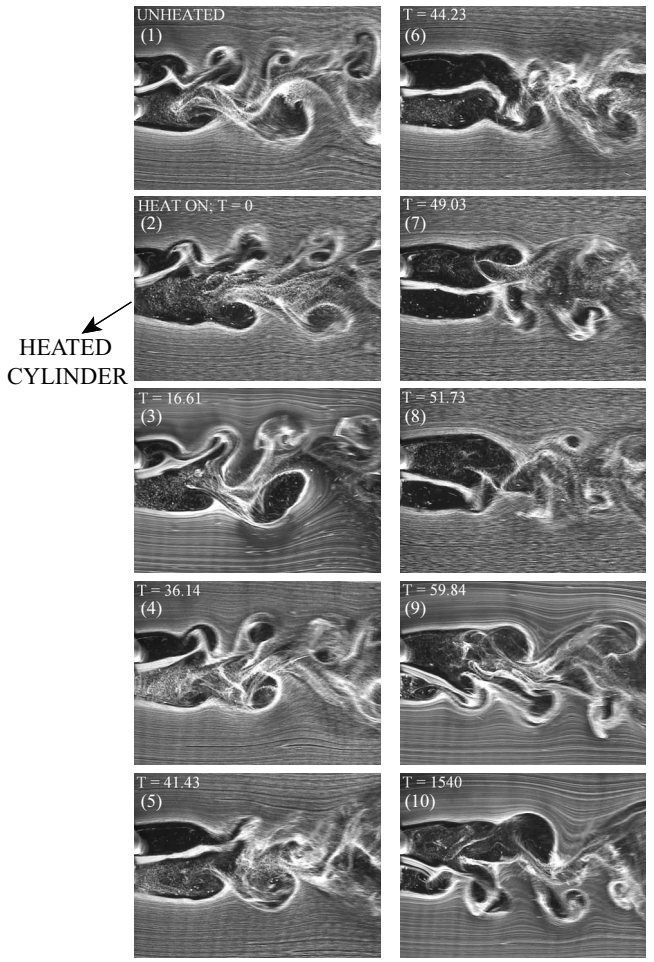

FIG. 11. Sequence of ten frames showing the effect of threshold heat release from one cylinder on the near-wake structure behind two cylinders at Re=350 and $S/D=1.7$. The heated cylinder on the right (looking downstream) is not visible due to the change in refractive index of water in the immediate vicinity of the heated cylinder.

shows the vorticity distribution behind two circular cylinders at a separation of $S/D=1.7$ and Re=350. The figure shows two single snapshots of vorticity distributions in shear layers

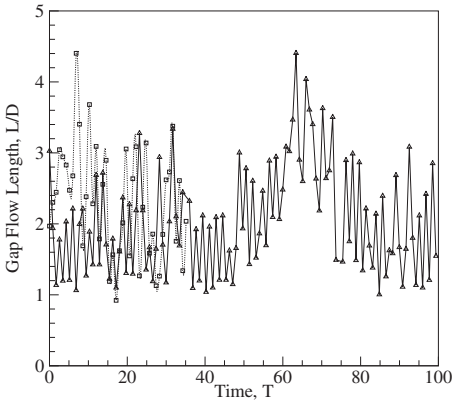

FIG. 12. Evolution of gap-flow length at Re=350 and $S/D=1.7$. Solid line—with threshold heat release, heat ON at $T=40.22$; dotted line—with no heat release, gap flow stably switched.

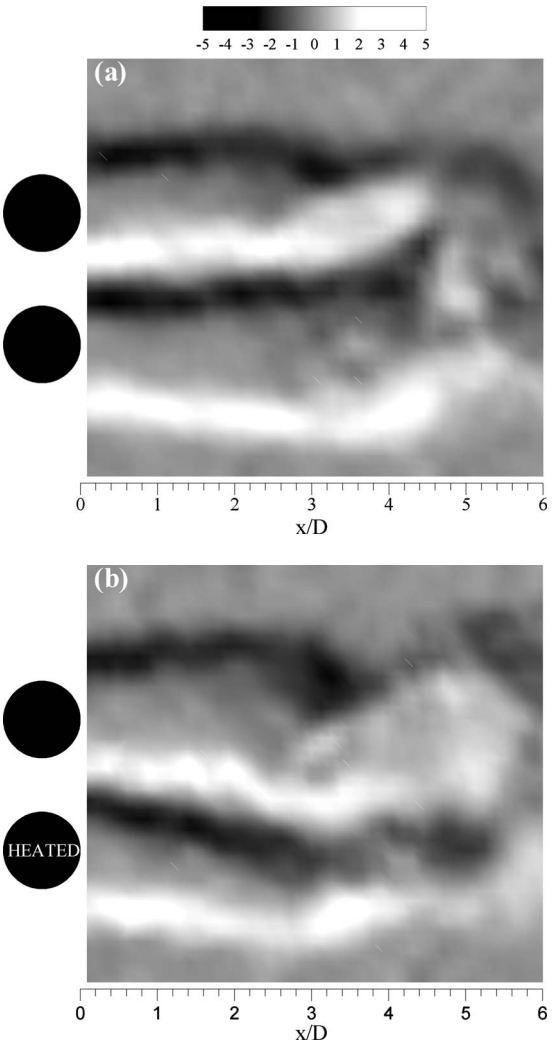

FIG. 13. PIV measurements of spanwise vorticity distribution, $\omega_z D/U_\infty$, at $S/D=1.7$ and Re=350. (a) Unheated cylinders; (b) right cylinder heated at threshold value. Flow is from left to right.

in two cases to illustrate their structure for a typical case. The vorticity has been nondimensionalized by the diameter of the cylinder, D, and the free-stream velocity, U_∞, as $\omega_z D/U_\infty$. The Fig. 13(a) shows the vorticity distribution with two unheated cylinders. The four shear layers coming off the two cylinders are clearly visible. The two shear layers in between the two cylinders constitute the gap flow. The gap flow is deflected to the left in this case. Figure 13(b) shows the vorticity distribution when the threshold value of the heat release was turned ON and the gap flow was forced to deflect toward the right cylinder.

The effect of the heat release on the gap flow and hence on the near-wake structure that was observed at Re=350 and $S/D=1.7$ was also observed at Re=250 and 450 at same spacing. The threshold value of the heat release depended on the value of the Reynolds number. Table II lists the threshold heat release, Q, values at the three Reynolds numbers studied and $S/D=1.7$. The value of the average Nusselt number for the heated cylinder in the present experiments at $S/D=1.7$ was calculated from the data at the threshold heat release condition and three Reynolds numbers. The Nusselt number

TABLE II. Table summarizing the data at $S/D=1.7$ for threshold heat release, Q, measured average temperature difference between the cylinder surface and free stream, measured Nusselt number, Nu, and expected value of Nu for single cylinder calculated from Eq. 7.52 of Ref. [19].

Re	Q (W) (threshold)	Measured (T_W-T_∞) (°C)	Nu	Single isolated cylinder expected Nu
250	57.6	10	14.7	16.3
350	162.5	20	20.7	19
450	233	24	24.8	21.4

is defined as $\bar{h}D/k$ where $\bar{h}$ is the convective heat transfer coefficient and k is the thermal conductivity of water. The calculated values of Nu in the present experiments were compared with the expected value of Nu for an isolated cylinder case. The expected values for isolated cylinder case were calculated using Eq. 7.52 from the book by Incropera [19]. The equation relates average Nu with the Re and Prandtl number, Pr, as $\mathrm{Nu}=C\mathrm{Re}^m\mathrm{Pr}^{1/3}$. The values of the constants C and m are 0.683 and 0.466, respectively, for the range of Reynolds numbers studied. The measured values of Nu in the present experiments are tabulated in the Table II along with the expected values for the isolated cylinder for comparison purposes.

In summary, the effect of heat release from one of the cylinders at $S/D=1.7$ has been the locking of the gap flow toward the heated cylinder at threshold value. In the case of unheated cylinders, it was observed by Kim and Durbin [7] that the gap flow is always directed toward the cylinder having lower base pressure. They measured the base pressures on both the cylinders simultaneously and found that the cylinder which had a narrow wake behind it always had lower base pressure compared to the other cylinder with wider wake. Admittedly, the present observations and measurements do not provide a clear physical reason for gap-flow deflection toward the heated cylinder. A possible explanation of the deflection of the gap flow toward the heated cylinder in the present experiments is perhaps that the deflection occurs due to lowering of the base pressure behind the heated cylinder (not investigated in the present experiments). When the mean base pressure behind the heated cylinder is reduced to values suitably lower than the one behind the unheated cylinder the gap flow will be deflected from the high base pressure region to the lower base pressure region. The effect of heat release is to lower the viscosity of water in the boundary layer over the cylinder which in turn lowers the diffusion of vorticity in the layer. The imbalance created between the diffusion, production, and advection of vorticity in the boundary layer due to turning ON the heat release can alter the location of separation point of the shear layers whose effect can get manifested in the base pressure values. A detailed experimental study of the effect of heat release on the base pressure values on a single cylinder can considerably help in testing our proposed hypothesis and in better understanding the physics of the gap-flow deflection in the present experiments.

The study conducted at $S/D=3.0$ at the three Reynolds numbers of 250, 350, and 450 showed the well known [6] pattern of in-phase (asymmetrical) and antiphase (symmetrical) vortex streets from the two cylinders without any heat release. The heat release, which was gradually increased, from one of the cylinders did not produce any visible changes in the vortex shedding patterns, i.e., combinations of in-phase and antiphase patterns were still observed. Figure 14 shows the two observed vortex shedding patterns with no heat release at Re=350.

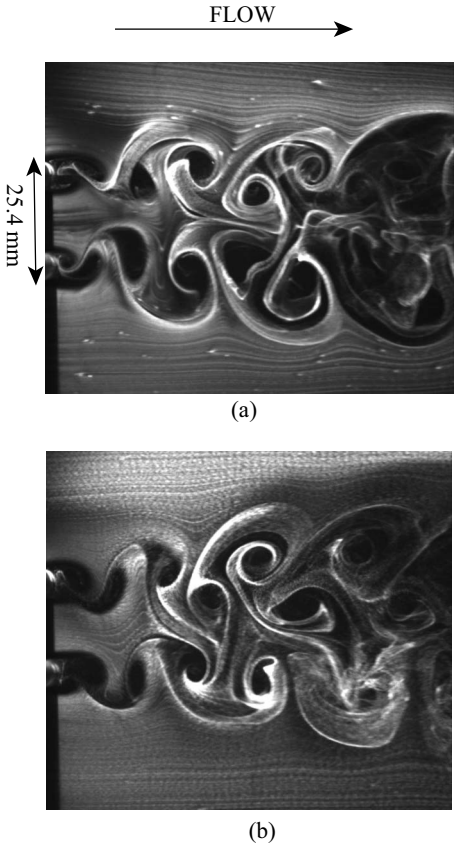

FIG. 14. Antiphase (symmetrical) and in-phase (asymmetrical) vortex shedding patterns behind two cylinders at Re=350 and $S/D=3.0$. (a) Antiphase shedding; (b) in-phase shedding.

The vortex shedding pattern observed at spacing of $S/D=1.1$ resembles the vortex shedding pattern behind a single bluff body [6] at the Reynolds numbers studied. There is a thin gap flow (also called as the gap-bleeding flow) between the cylinders. The role of gap-bleeding flow is well documented in the work of Wang and Zhou [6]. In the present experiments, the gap-bleeding flow was wrapped around one of the cylinders and rarely shifted from one cylinder to the other. The overall vortex shedding pattern appears unchanged whether the gap-bleeding flow is close to one or the other cylinder. The heat release produced the same effect on the gap-bleeding flow as it did on the gap flow at $S/D=1.7$, i.e., the heated cylinder attracted the gap-bleeding flow toward itself. Figure 15 shows the effect of heat release on the gap-bleeding flow at $S/D=1.1$ and Re=350. Figure 15(a) shows the case of two unheated cylinders at Re=350 with the gap-bleeding flow biased toward the left cylinder. The gap-bleeding flow closely wraps around the left cylinder and merges with the outer shear layer of this cylinder. The heat

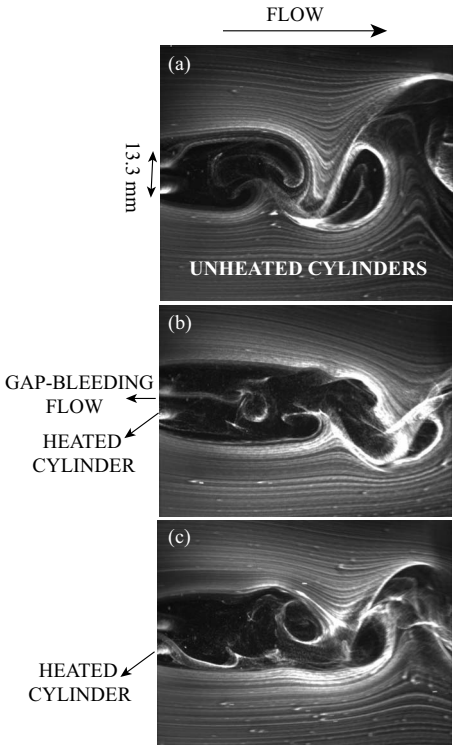

FIG. 15. Effect of threshold heat release on gap-bleeding flow at Re=350 and $S/D=1.1$. (a) Unheated cylinders: gap bleeding biased toward left cylinder; (b) right cylinder heated: gap-bleeding flow straight and switching toward right cylinder. (c) Right cylinder heated: gap-bleeding flow forced toward heated cylinder.

release (~80 W) was then turned ON from the right cylinder and the gap-bleeding flow started responding to it. Figure 15(b) shows the instant when the gap-bleeding flow was relatively straight, and in Fig. 15(c) it is completely biased toward the right heated cylinder. The undeflected gap-bleeding flow as shown in Fig. 15(b) clearly results in a longer vortex formation region relative to the biased gap-bleeding flow cases. The undeflected gap-bleeding flow results in unstable symmetric vortex shedding as was pointed out by Wang and Zhou [6]. The amount of heat release required to force the gap-bleeding flow to shift from unheated cylinder to the heated cylinder at two other Reynolds numbers of 250 and 450 was approximately the same at this spacing.

IV. CONCLUSIONS

The effect of heat release from one of the cylinders in a side-by-side configuration on the near-wake structure was studied at three spacings, $S/D=1.1$, 1.7, and 3.0 and three Reynolds numbers of 250, 350, and 450. The flow visualization was done using the hydrogen bubble technique and quantitative vorticity measurements were done using PIV. The spacing ratio of $S/D=1.7$ with no heat release shows the well-known bistable wake. The stability of the two stable states with no heat release was studied by observing the response of the wake to an external perturbation. The perturbation has the effect of sometimes stably switching the gap flow. It is observed that perhaps the near-wake structure is more stable at lower Reynolds numbers and this is consistent with the observation of other researchers. The near-wake structure shows oscillations as the perturbation is applied. The gap-flow length shows a sudden decrease as the perturbation is applied and then returns to its original oscillating behavior.

The effect of heat release in one of the cylinders showed that at a threshold value of heat release, the gap-flow deflects toward the heated cylinder resulting in a *stable* wake structure with a relatively narrow wake behind the heated cylinder. The forced switching of the gap flow toward the heated cylinder at threshold value of heat release occurs over a time scale ($T\sim 50$) which is an order of magnitude greater than the time scale for natural switching of the gap flow with unheated cylinder ($T\sim 5$). The threshold value of heat release depends on the Reynolds number and shows an increasing trend with Reynolds number. It is hypothesized that the switching of the gap flow with threshold heat release occurs due to lowering of the base pressure behind the heated cylinder. The two cylinder configuration at spacing ratio of $S/D=1.1$ behaves as a single bluff body with a very thin gap-bleeding flow between the two cylinders. The heat release has a similar effect on the gap-bleeding flow as in the case of $S/D=1.7$. The gap-bleeding flow deflects toward the heated cylinder at a threshold value of heat release—which remains approximately constant with Reynolds number in the present experiments. The experiments at spacing ratio of $S/D=3.0$ show the two in-phase (asymmetrical) and antiphase (symmetrical) configurations of the wake structure. The heat release did not have any visual effect on the near-wake structure at the spacing ratio of $S/D=3.0$ in the ranges of Reynolds numbers studied.

ACKNOWLEDGMENTS

The authors would like to acknowledge the support provided by the National Science Foundation through the MRI Grant No. CMMI-0723094. The purchase of the PIV system was made possible through this grant.

[1] A. Roshko, J. Wind Eng. Ind. Aerodyn. **49**, 79 (1993).
[2] P. W. Bearman and A. J. Wadcock, J. Fluid Mech. **61**, 499 (1973).
[3] M. M. Zdrakovich, J. Fluids Eng. **99**, 618 (1977).
[4] C. H. K. Williamson, J. Fluid Mech. **159**, 1 (1985).
[5] D. Sumner, S. S. T. Wong, S. J. Price, and M. P. Päidoussis, J. Fluids Structures **13**, 309 (1999).
[6] Z. J. Wang and Y. Zhou, Int. J. Heat Fluid Flow **26**, 362 (2005).
[7] H. J. Kim and P. A. Durbin, J. Fluid Mech. **196**, 431 (1988).

[8] H. M. Spivac, J. Aeronaut. Sci. **13**, 289 (1946).
[9] S. Ishigai, E. Nishikawa, K. Nishmura, and K. Cho, Bull. JSME **15**, 949 (1972).
[10] R. N. Kieft, C. C. M. Rindt, and A. A. van Steenhoven, Exp. Therm. Fluid Sci. **19**, 183 (1999).
[11] A. B. Wang, T. Zdenek, and K. C. Chia, Phys. Fluids **12**, 1401 (2000).
[12] W. J. P. M. Mass, C. C. M. Rindt, and A. A. van Steenhoven, Int. J. Heat Mass Transfer **46**, 3069 (2003).
[13] J. M. Shi, D. Gerlach, M. Breuer, G. Biswas, and F. Durst, Phys. Fluids **16**, 4331 (2004).
[14] R. Maosheng, C. C. M. Rindt, and A. A. van Steenhoven, J. Fluid Mech. **566**, 195 (2006).
[15] A. I. Fedorchenko, Z. Trávníĉek, and A. B. Wang, Phys. Fluids **19**, 051701 (2007).
[16] T. S. Pottebaum, Ph.D. thesis, Aeronautics, California Institute of Technology, 2003.
[17] V. T. Morgan, Adv. Heat Transfer **11**, 199 (1975).
[18] See EPAPS Document No. E-PLEEE8-80-024912 for movies on the effect of external perturbation at Re=250, 350, and 450 and $S/D=1.7$ with no heat release. For more information on EPAPS, see http://www.aip.org/pubservs/epaps.html.
[19] F. P. Incropera, D. P. Dewitt, T. L. Bergman, and A. S. Lavine, *Fundamentals of Heat and Mass Transfer*, 6th ed. (Wiley, New York, 2007).